

THE LUMINOSITIES, SIZES AND VELOCITY DISPERSIONS OF BRIGHTEST CLUSTER GALAXIES: IMPLICATIONS FOR FORMATION HISTORY

MARIANGELA BERNARDI¹, JOSEPH B. HYDE¹, RAVI K. SHETH¹, CHRIS J. MILLER², AND ROBERT C. NICHOL³

ABSTRACT

We find that the size-luminosity relation of early-type Brightest Cluster Galaxies (BCGs), $R_e \propto L^{0.92}$, is steeper than that for the bulk of the early-type galaxy population, for which $R_e \propto L^{0.62}$. This is true if quantities derived from either deVaucouleur or Sersic fits to the surface brightness profiles are used. This difference is *not* due to contamination from intra-cluster light. In addition, when placed on the Fundamental Plane defined by the bulk of the early-type population, early-type BCGs show only a small offset, but considerably smaller scatter. The larger than expected sizes of BCGs, and the increased homogeneity, are qualitatively consistent with models which seek to explain the colors of the most massive galaxies by invoking dry dissipationless mergers, since dissipation tends to reduce the sizes of galaxies, and wet mergers which result in star formation would tend to increase the scatter in luminosity at fixed size and velocity dispersion. Furthermore, BCGs define the same $g - r$ color-magnitude relation as the bulk of the early-type population. If BCGs formed from dry mergers, then BCG progenitors lay redward of this relation, suggesting that they hosted older stellar populations than typical for their luminosities. Our findings have two consequences. First, the $R_e - L$ relation of the bulk of the early-type galaxy population exhibits some curvature: the most luminous galaxies tend to have larger sizes than expected from the $R_e \propto L^{0.62}$ scaling. This is a consequence of the fact that an increasing fraction of the most luminous galaxies are BCGs. The second consequence is suggested by the fact that, despite following a steeper size-luminosity relation, BCGs tend to define a tight relation between dynamical mass $R_e \sigma^2 / G$ and luminosity. As a result, they define a shallower $\sigma - L$ relation than the bulk of the early-type galaxy population. This shallower relation suggests there may be curvature in the correlation between black hole mass and velocity dispersion; simple extrapolation of the $M_{\text{BH}} - \sigma$ relation to large σ will underestimate M_{BH} .

Subject headings: galaxies: elliptical — galaxies: evolution — galaxies: fundamental parameters — galaxies: photometry — galaxies: stellar content

1. INTRODUCTION

Understanding why massive early-type galaxies are red and dead has proved to be difficult; the problem is to arrange for star formation to occur at higher redshift than the actual assembly of the stars into a single massive galaxy. The most recent galaxy formation models arrange for this to happen by a combination of two processes: dry mergers and AGN feedback (Hopkins et al. 2005; Croton et al. 2005; De Lucia et al. 2005; Robinson et al. 2006; Bower et al. 2006). The dry merger hypothesis assumes that the assembly of massive galaxies occurs by merging smaller progenitor systems of old stars without additional star formation (which would otherwise lead to bluer colors). This happens either because the merging units were themselves gas poor, or because AGN feedback has prevented the hot gas reservoirs of the progenitors from cooling and forming stars after the merger. Together, these processes allow massive galaxies to be built from smaller systems while still remaining red.

The dry merger hypothesis is most necessary for the most massive galaxies. These tend to be the brightest galaxies in clusters (BCGs). Therefore, we have initiated

a study of objects which are identified as Brightest Cluster Galaxies in the C4 cluster catalog of Miller et al. (2005). This catalog is complete out to $z = 0.15$, contains about 700 BCGs, and will contain about 1500 BCGs by Fall 2006.

Our primary focus will be the sizes of these BCGs, although we also study a number of other scaling relations. This is because, in a ‘wet’ merger, gas from the merging components is able to dissipate energy, cool, contract and eventually make new stars. Dry mergers on the other hand have no energy loss mechanism; having suffered less dissipation, their stellar components are not as centrally contracted, so the optical sizes of dry merger products are expected to be larger than if the mergers were wet (e.g. Kormendy 1989).

Section 2 describes the sample and provides a brief summary of our fits to the photometric properties of BCGs. Details are provided in Hyde et al. (2006). These new fits were necessary, as the SDSS photometric reductions of objects in crowded fields suffer from sky subtraction problems (e.g. Hyde et al. 2006; Lauer et al. 2006). In Section 3 we compare a variety of BCG scaling relations to those of the bulk of the early-type galaxy population. This section shows that BCGs define a steeper size-luminosity relation than does the bulk of the early-type galaxy population; that although BCGs have larger than expected sizes, they still define a tight relation between luminosity and dynamical mass $R\sigma^2/G$, and so the $\sigma - L$ relation of BCGs curves away from the power-law scaling defined by the bulk of the early-type galaxy pop-

¹Department of Physics and Astronomy, University of Pennsylvania, Philadelphia, PA 19104

²Cerro-Tololo Inter-American Observatory, NOAO, Casilla 603, La Serena, Chile

³Institute of Cosmology and Gravitation (ICG), Mercantile House, Hampshire Terrace, University of Portsmouth, Portsmouth, PO1 2EG, UK

ulation. It also shows the location of BCGs in the same Fundamental Plane defined by normal early-type galaxies, and shows that they define the same color-magnitude relation as normal early-type galaxies. The Appendix presents a comparison with the color-magnitude relation predicted by semi-analytic galaxy formation models.

Section 4 studies two systematic errors which might have caused the steeper $R_e - L$ relation we see, and concludes that they are not to blame. The first possibility is that the deVaucouleur fit is systematically worse for BCGs than it is for the bulk of the population. The second possibility is more subtle. Galaxy clusters contain a substantial population of stars which are not associated with a galaxy (e.g. Gonzalez et al. 2005; Zibetti et al. 2005). So it is not unreasonable to ask if this intracluster light is contaminating our estimates of the sizes and luminosities of BCGs, and hence the inferred $R_e - L$ and $\sigma - L$ relations.

At the very largest luminosities ($M_r < -23.5$), the $R_e - L$ relation of the bulk of the early-type galaxy population appears to curve upwards toward larger sizes from the $R_e \propto L^{0.62}$ scaling. If an increasing fraction of these objects are BCGs, then this curvature is not unexpected in view of our finding that BCGs follow a steeper size-luminosity relation. Section 5 presents evidence from SDSS imaging that, at large luminosities, an increasing fraction of galaxies are indeed BCGs.

A final section summarizes our findings and discusses the implications for galaxy formation models, and for studies which seek to estimate the mass of a supermassive black hole from the stellar velocity dispersion of the bulge which surrounds it. Where necessary, we assume a flat cosmological model with $\Omega_0 = 0.3$, $\Lambda = 1 - \Omega_0$ and $H_0 = 70h_{70} \text{ km s}^{-1} \text{ Mpc}^{-1}$.

2. SAMPLE SELECTION AND FITS TO LIGHT PROFILES

We have selected the objects identified as BCGs in the C4 cluster catalog of Miller et al. (2005). This catalog was based on the Second Data Release of the SDSS: DR2. Of the 748 BCGs in the catalog, spectra are available for 580 (fiber collisions mean some BCGs were missed). Some of these are duplicates, and the number which are matched to a parent catalog based on SDSS DR4 is 403. Of these, 286 have $M_r < -21$ (we believe less luminous BCGs are likely to be misidentifications), have SDSS reported velocity dispersions, and have at least 10 other luminous galaxies ($M_r < -21$) within $1h^{-1}\text{Mpc}$. (The SDSS does not estimate velocity dispersions from spectra which have strong emission lines, so our requirement that the SDSS reports a velocity dispersion means that the objects we select are almost certainly not AGN. Removing the final cut on ‘richness’ increases the sample of BCGs to 324, but does not change the results which follow.)

Visual inspection of the SDSS images of these objects shows that 25% actually have spiral arms (the absence of emission lines in the spectra of these objects is presumably because the SDSS fiber, with a radius of 1.5’ arcsec, only sees the inner bulge). In what follows, we will be careful to distinguish the scaling relations of the ~ 215 genuine early-type BCGs from the rest.

It happens that BCGs are a class of object for which the SDSS photometric reductions are particularly unreliable: the reported magnitudes are in error by far more

than the quoted 0.02 mags, with some discrepancies as large as 1 mag (Lauer et al. 2006). This is due to a combination of factors: because BCGs are often in crowded fields, the SDSS reductions tend to overestimate the sky level. This results in underestimates of the BCG magnitude and half-light radius, which are particularly severe for BCGs with large half-light radii. In addition, the surface brightness distributions of BCGs do not always follow pure single component deVaucouleurs profiles, which the SDSS reductions assume. For these reasons, we have performed our own photometric reductions, and examined the image of each BCG by eye. A more detailed discussion of the various issues involved is provided by Hyde et al. (2006), whose results we use below.

The most important finding of this reanalysis of BCG photometry is that there appear to be two classes of early-type BCG light profiles. Examples of these two types are shown in Figures 1 and 2. The first type is well fit by a single component deVaucouleurs profile, whereas the second is not. This second type of profile is similar to that associated with cD galaxies. Section 4 discusses these two profile types in more detail. Meantime, we will be careful to treat these two populations separately in what follows.

3. BCG SCALING RELATIONS

3.1. The size-luminosity relation of BCGs

Figure 3 shows the correlation between luminosity and half-light radius for the C4 BCGs: diamonds represent spiral morphologies, and filled circles represent E/S0s. Solid line shows the $R_e - L$ relation defined by the bulk of the early-type galaxy population—BCGs clearly define a steeper relation. (The steeper relation is also seen if we

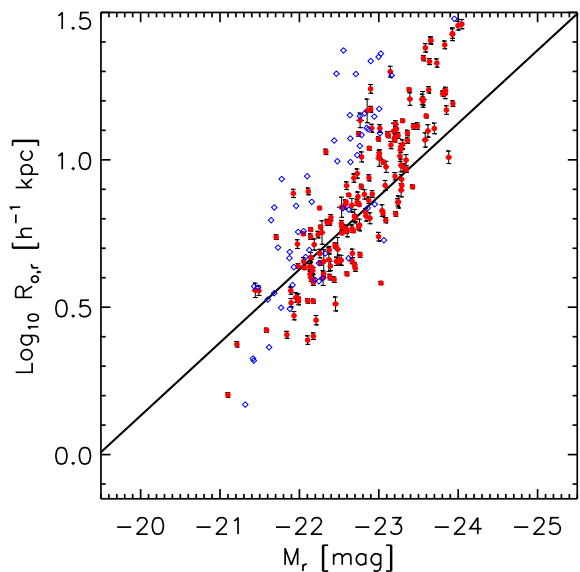


FIG. 3.— C4 BCGs define a steeper size-luminosity relation (symbols) than does the bulk of the early-type galaxy population (solid line). Open diamonds and filled circles represent BCGs with spiral and E/S0 morphologies, respectively. In what follows, we only consider the E/S0 objects.

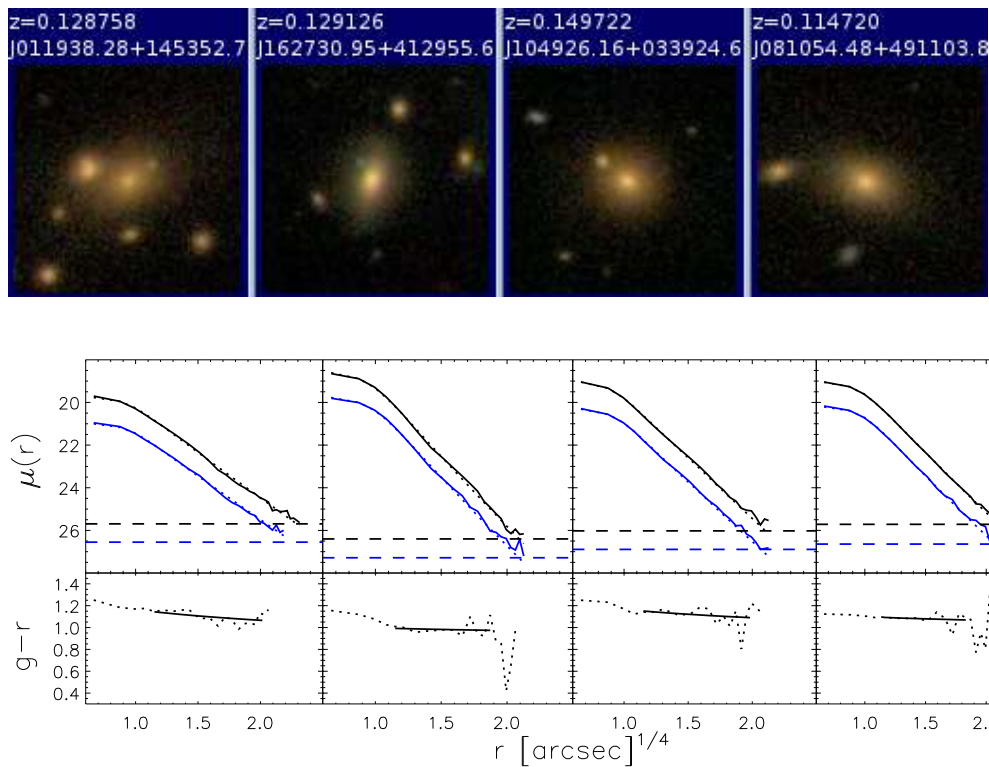


FIG. 1.— Images (top) and surface brightness profiles (bottom) for a set of C4 BCGs which are well fit by a single deVaucouleur profile. The fit is good in both the g and r bands. Horizontal dashed lines show one percent of the sky brightness in the two bands. Bottom half of bottom panels shows the associated $g - r$ color gradient—the gradient is expected to be weak if the formation was dominated by mergers.

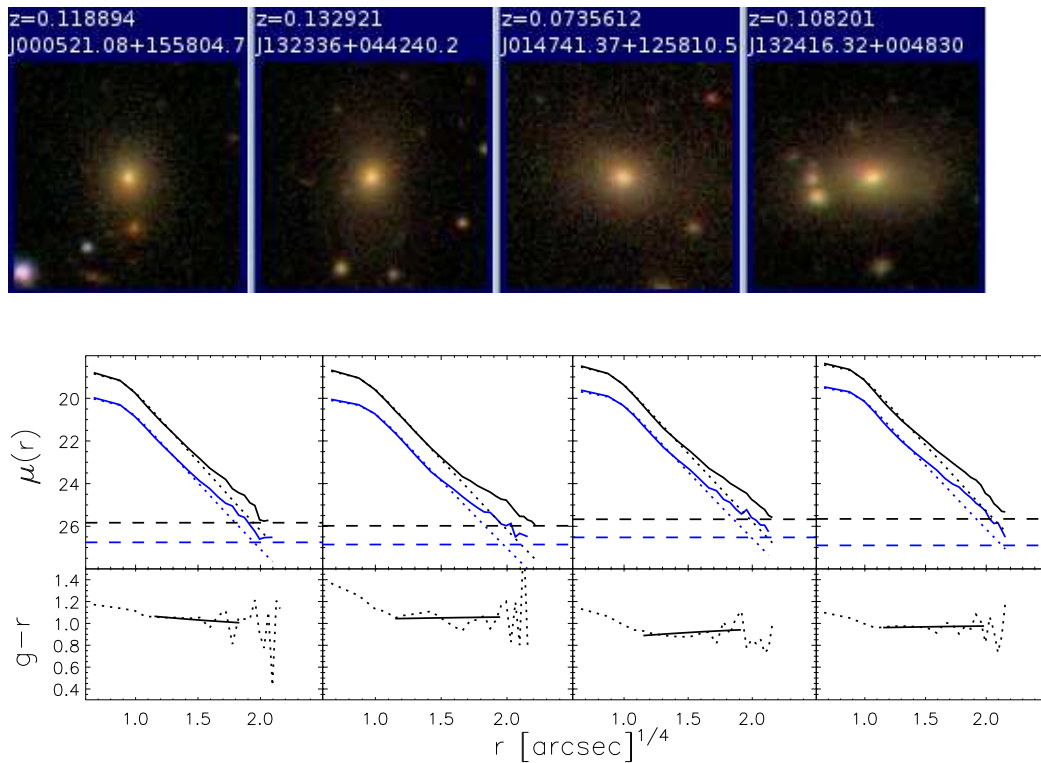


FIG. 2.— Images (top) and surface brightness profiles (bottom) for a set of C4 BCGs which are not well fit by a deVaucouleur profile. The deviation is strongest at large radii (faint surface brightness). Although Sersic profiles provide better fits, Gonzalez et al. (2006) show that the sum of two deVaucouleur components generally provide an even better description of most such profiles.

use the original SDSS photometric reductions which we believe to be incorrect.) In what follows, we focus on the early-type BCGs, but note that the spiral BCGs define an $R_e - L$ relation that is at least as steep.

Figure 4 shows the $R_e - L$ relation for the early-type BCGs, now subdivided by whether or not the surface brightness profile is well fit by a single deVaucouleurs profile (red) or not (green). Jagged solid line shows the average size of the BCGs which are well fit by deVaucouleur profiles in a few bins in luminosity, and dashed line shows a power-law fit to the size-luminosity relation for these BCGs:

$$\langle \log_{10} R_e | M_r \rangle = -0.92 M_r / 2.5 - 7.50. \quad (1)$$

This fit should be compared to the straight solid line which shows the scaling which provides a good description of the bulk of the early-type galaxy population:

$$\langle \log_{10} R_e | M_r \rangle = -0.62 M_r / 2.5 - 4.83. \quad (2)$$

Clearly BCGs define a steeper relation—they have larger sizes than do normal early-type galaxies of similar luminosity. This trend is consistent with the hypothesis that BCGs have formation histories with less dissipation than the bulk of the early-type population.

3.2. The mass-luminosity relation

The larger than expected sizes have interesting consequences. If these objects are virialized, then one expects a relatively tight correlation between luminosity and the

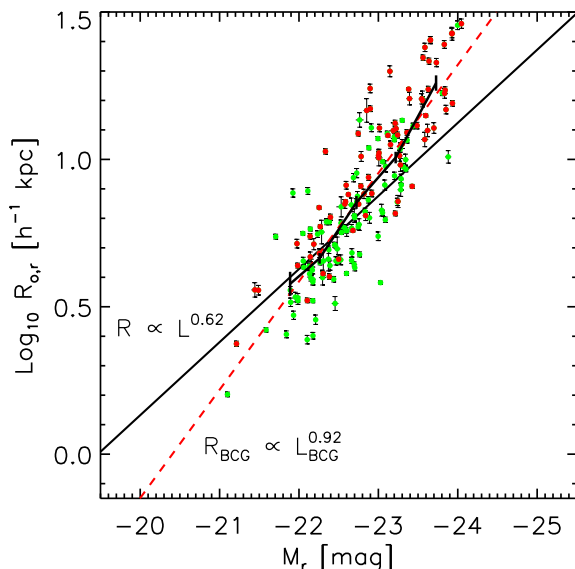


FIG. 4.— Early-type C4 BCGs define a steeper size-luminosity relation (symbols and dashed line) than does the bulk of the early-type galaxy population (solid line). The larger sizes of BCGs are consistent with the hypothesis that BCGs formed from dry mergers. Red and green symbols represent objects which are well described by a deVaucouleurs profile, and those which are not.

dynamical mass $\propto R_e \sigma^2 / G$. Figure 5 shows that this correlation is indeed rather tight—the inset shows that BCGs define a tighter relation than does the bulk of the early-type galaxy population. This smaller scatter is also consistent with dry-merger formation histories; one might have expected ‘wet’ mergers to result in star formation, which would increase the scatter in luminosities at fixed dynamical mass.

3.3. The velocity dispersion-luminosity relation

If the $R_e - L$ relation for BCGs is steeper than for the bulk of the early-type galaxy population, then the tight correlation between L and dynamical mass shown in Figure 5 suggests that the $\sigma - L$ relation for BCGs must be shallower. Figure 6 shows that this does appear to be the case. Once again, the solid line shows the relation for the full sample, dashed line shows a fit to the objects which are single component deVaucouleur profiles (red symbols), and green symbols show the other BCGs. A running average over small bins in luminosity shows evidence for curvature in the $\sigma - L$ relation, in the sense that velocity dispersion increases only weakly with luminosity once $\sigma \geq 250$ km/s.

3.4. The Fundamental Plane

Numerical simulations of a dry merger scenario suggest that the final object will remain on the Fundamental Plane defined by the bulk of the early-type population (Boylan-Kolchin et al. 2006). Figure 7 shows the location of the C4 BCGs in the Fundamental Plane defined by the bulk of the early-type galaxy population. The BCGs are slightly offset (0.013 dex) from this plane. However, the inset shows that the scatter around this Plane is significantly reduced—the scatter orthogonal to the Plane decreases from 0.057 dex to 0.04 dex. This reduced scatter for BCGs is consistent

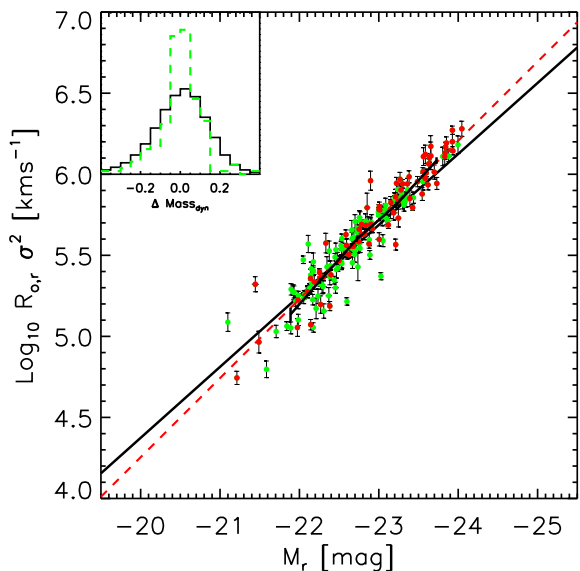


FIG. 5.— BCGs define an even tighter correlation between dynamical mass $R_e \sigma^2$ and luminosity than does the bulk of the early type galaxy population. This is not unexpected if BCGs formed by dry mergers.

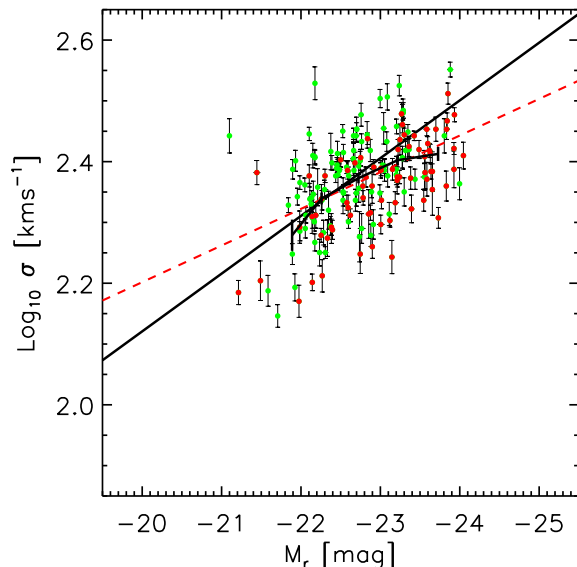


FIG. 6.— The $\sigma - L$ relation of C4 BCGs appears to flatten at high luminosities. This may be due to dry merger formation histories—the smaller dissipation in a dry merger results in larger sizes and smaller velocity dispersions. This curvature may be related to studies of curvature in the $M_{\text{BH}} - \sigma$ relation.

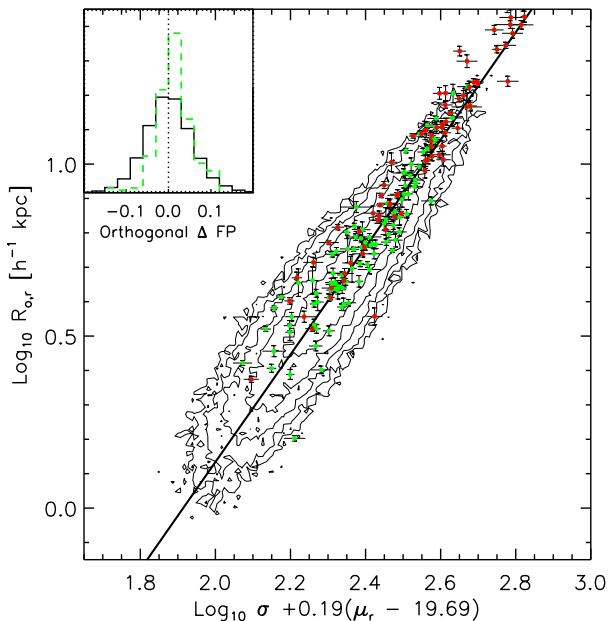


FIG. 7.— Location of C4 BCGs (symbols) with respect to the Fundamental Plane defined by the bulk of the early-type galaxy population (contours). Inset shows that BCGs are distributed more tightly around this FP than the bulk of the early-type galaxy population: the rms scatter is 0.04 dex compared to 0.057 dex. Similar results are obtained in the other SDSS bands.

with a dry merger formation history—even a small amount of star formation associated with a wet merger has the potential to change the surface brightnesses significantly, resulting in increased scatter about the Plane.

3.5. The color-magnitude relation

Early-type galaxies define a tight correlation between color and luminosity. Figure 8 shows that BCGs follow the same correlation, though with slightly smaller scatter. The Appendix presents a comparison with the color-magnitude relation predicted by semi-analytic galaxy formation models. The models suggest that BCGs should lie slightly blueward of the relation defined by the bulk of the population—an effect which is not seen in Figure 8.

Whereas the luminosity of an object formed from a dry merger is expected to be the sum of the luminosities of the objects involved in the merger, the merger is not expected to change the color (there being no associated star formation). Therefore, if BCGs formed from dry mergers, then the fact that they define the *same* color-magnitude relation as the bulk of the population suggests that the progenitors of BCGs were red for their luminosities. Objects which lie redward of the color-magnitude relation are expected to be older (Kodama et al. 1998; Bernardi et al. 2005). Thus, Figure 8 is not inconsistent with the expectation that the oldest stars in a halo find their way to the bottom of the potential well—the location of which is often traced by the BCG.

Although we have not included a figure showing this, we have found that BCGs also lie on the same σ -color

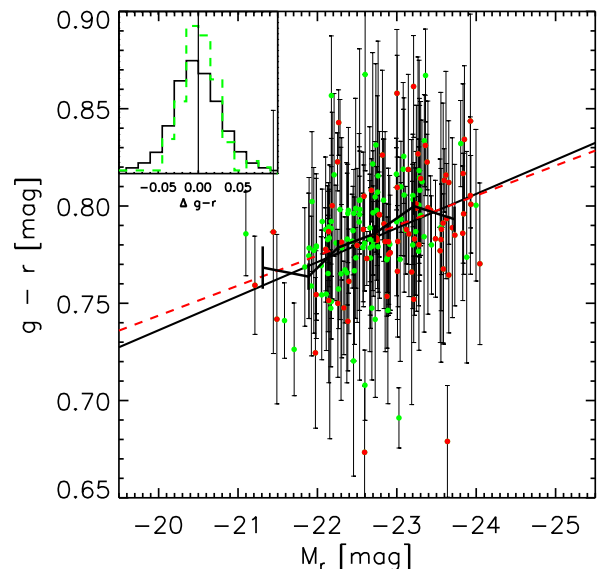


FIG. 8.— Location of C4 BCGs (symbols) with respect to the color-magnitude relation defined by the bulk of the early-type galaxy population (solid line). Dashed line shows a linear fit of color as a function of absolute magnitude, and jagged line with error bars shows the mean color in a few bins in luminosity. Inset shows that BCGs are not offset from the relation defined by the bulk of the population, though the relation they define is slightly tighter.

correlation as the bulk of the early-type population. This is consistent with a model in which the color is not altered by the merger, and the change to σ is also weak (recall Figure 6 suggests that dry mergers do not change σ as much as they change L).

4. TESTS OF SYSTEMATIC EFFECTS

This section studies two possible sources of systematic trends and concludes that they do not cause the steeper $R_e - L$ relation we see in our early-type BCG sample.

4.1. Sersic profile fits

We have considered the possibility that the steeper $R_e - L$ relation we see arises because the deVaucouleur profile provides a systematically worse description of early-type surface brightness profiles at large L . Figures 9–11 show results obtained from fitting Sersic profiles to the full early-type sample, as well as to the BCGs. Figure 9 shows that $n > 4$ at large L , indicating that the deVaucouleur profile ($n = 4$) is indeed systematically off at large L . It also shows that objects which we identified as potentially having two components (like those shown in Figure 2) tend to have large values of n . Figure 10 shows that, for those objects which we flagged as having two components, the luminosities and half-light radii derived from the Sersic fits tend to be substantially larger than when the fit is restricted to a deVaucouleur profile. In some cases the difference in total luminosity is as large as one magnitude—

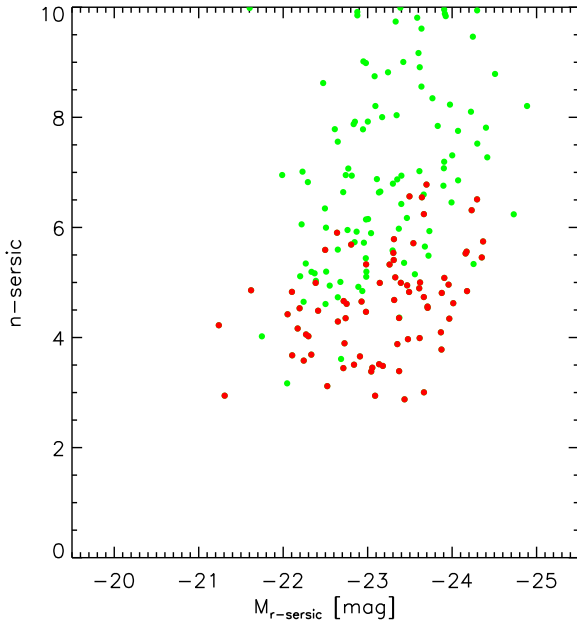


FIG. 9.— Correlation between Sersic parameter n and the total luminosity obtained from fitting the Sersic form to the surface brightness profiles (red symbols represent objects which are well fit by a single component deVaucouleur profile in the previous figures, and green symbols show the other early-type BCGs). A deVaucouleur profile has $n = 4$; notice that objects with large L tend to have large n , and that objects which show evidence for two components also tend to have large n .

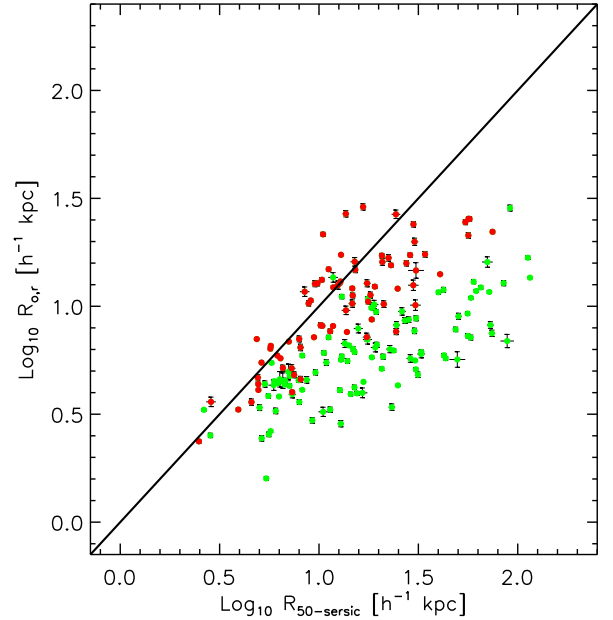
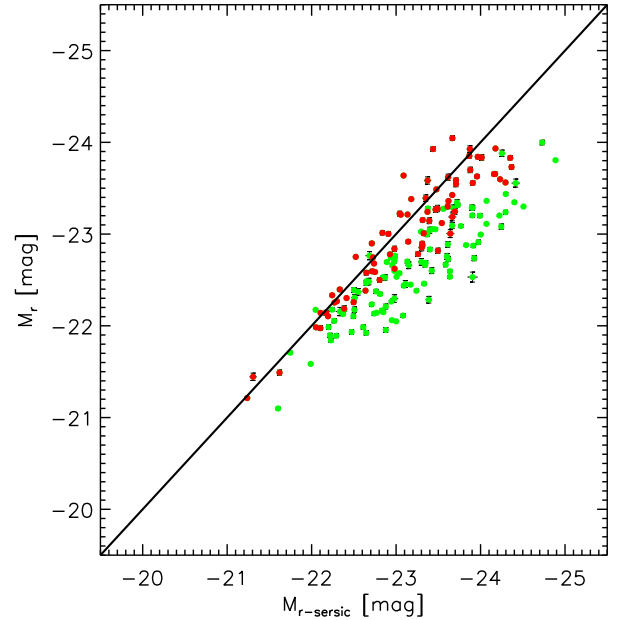


FIG. 10.— Comparison of total luminosities and half-light radii derived from deVaucouleur and Sersic fits to the surface brightness profiles. Red and green symbols represent objects which are well fit by deVaucouleur profiles and those which are not. For objects where the deVaucouleur profile is a poor fit (green symbols), the Sersic fits result in significantly larger total luminosities (top) and sizes (bottom).

this systematic difference dwarfs the 0.02 mag uncertainty usually quoted for SDSS photometry. Figure 11 shows the analog of Figure 4: the $R_e - L$ relation obtained from the Sersic profile fits. This illustrates that BCGs define a steeper relation than the bulk of the population even when parameters derived from Sersic fits are used.

4.2. The effect of intra-cluster light

The previous section showed that BCGs define a steeper size-luminosity relation than does the bulk of the early-type galaxy population. However, it is known that there is a component of the total luminosity of a cluster which is not associated with any particular galaxy in it: this intra-cluster light (ICL) tends to have a smooth profile centered on the cluster center. So it is natural to ask if this ICL profile is affecting our estimates of the sizes and luminosities of BCGs, thus altering the correlation between size and luminosity. This effect would be particularly severe for BCGs which lie at the cluster center. For such objects, it may be more reasonable to treat the surface brightness profile as the sum of two components, an inner one which represents the BCG itself, and an outer one which represents the ICL. This distinction is suggested by measurements of the velocity dispersion profiles in cD galaxies: whereas the velocity dispersion in the inner parts has values which are typical for massive galaxies, the velocity dispersion of the outer component rises significantly until it equals that of the cluster. This suggests that the ICL is a separate dynamical component from the BCG. Hence, to estimate

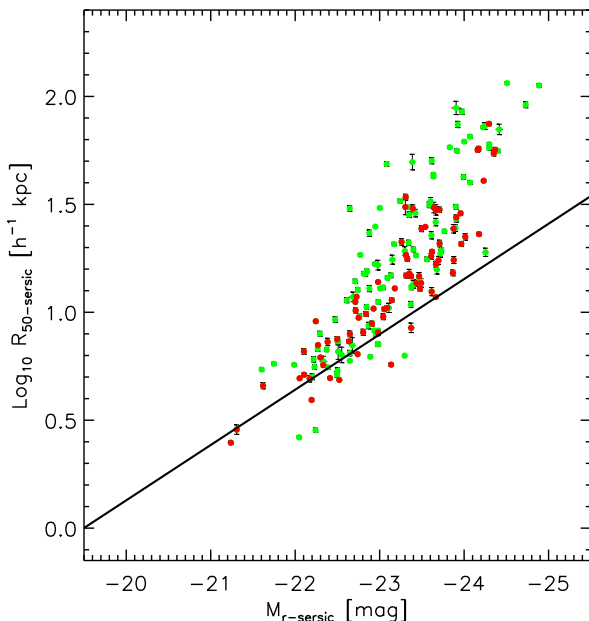


FIG. 11.— The $R_e - L$ relation obtained from fitting Sersic profiles to the surface-brightness distribution (compare Figure 3). Solid line shows the $R_e - L$ relation defined by the bulk of the early-type galaxy population; symbols show that C4 BCGs define a steeper relation (red symbols represent objects which are well fit by a single component deVaucouleur profile in the previous figures, and green symbols show the other early-type BCGs).

the size and luminosity of the BCG itself, it is necessary to identify the contribution to the surface brightness profile which is due to the ICL.

To estimate the effect of the ICL on our results, we have used two results from the recent literature. Zibetti et al. (2005) used a stacking technique to detect the ICL with high significance in SDSS clusters, and concluded that the ICL component has rather low surface brightness ($\mu_r > 25$ mag arcsec $^{-2}$): single SDSS exposures in the r -band are not sufficiently deep to detect it unambiguously, which is why a stacking analysis was required. This suggests that contamination from the ICL is unlikely to be a strong effect in our case. However, recent work by Gonzalez et al. (2005) shows that BCG light profiles deviate from a deVaucouleur fit at about the same surface brightness values (once the difference between their I band and our r band has been accounted for) at which we see deviations (c.f. Figure 2).

To check if the ICL is affecting our results, we made mock observations of BCGs of various luminosities as follows. For a given BCG luminosity, we require the half-light radius to satisfy $R_e \propto L^{0.62}$. We use this size and luminosity to generate a deVaucouleurs surface brightness profile. To this profile we add an ICL component, the parameters of which are motivated by the study of Zibetti et al.. Namely, the ICL component is modeled as a second deVaucouleurs profile, with the same integrated luminosity as the first component, but with half-light radius twenty times larger. We then fit the summed image with a single component deVaucouleurs profile (since this is, in effect, what the SDSS pipeline does), and record the best-fit values of luminosity and half-light radius. Upon repeating this procedure for a range of luminosities, we can compare the $R_{\text{BCG+ICL}} - L_{\text{BCG+ICL}}$ relation with the input one.

In general, the ICL component tends to increase *both* the size and the total luminosity of the BCG. Our experiments indicate that the net effect of the ICL is to move the BCG along the $R_e - L$ relation. Therefore, we find that the ICL component does not lead to a steepening of the $R_e - L$ relation. This conclusion remains unchanged if we use Sersic profiles instead, or the particular choice of Petrosian quantities used by the SDSS. (Because the Petrosian quantities do not make strong assumptions about the profile shape, one might have thought that they were particularly well suited to this comparison. However, the Petrosian quantities output by the SDSS pipeline are neither seeing-corrected nor have the correct sky subtraction, making them less attractive.)

5. BCGS AND THE MOST LUMINOUS GALAXIES

Figure 12 shows that, at the largest luminosities, the size-luminosity relation of the bulk of the early-type galaxy population begins to curve upwards towards even larger sizes. Curvature in the $R_e - L$ relation for cluster ellipticals was recently noted by Cypriano et al. (2006). What causes this curvature? If we view the $R_e - L$ relation as a number weighted average of the normal and BCG relations, then this curvature may be interpreted as indicating that, compared to lower luminosities, a growing fraction of the objects at these large luminosities must be BCGs. Figure 13 suggests that this is indeed the case; it shows $1.5' \times 1.5'$ fields centered on a random selection of

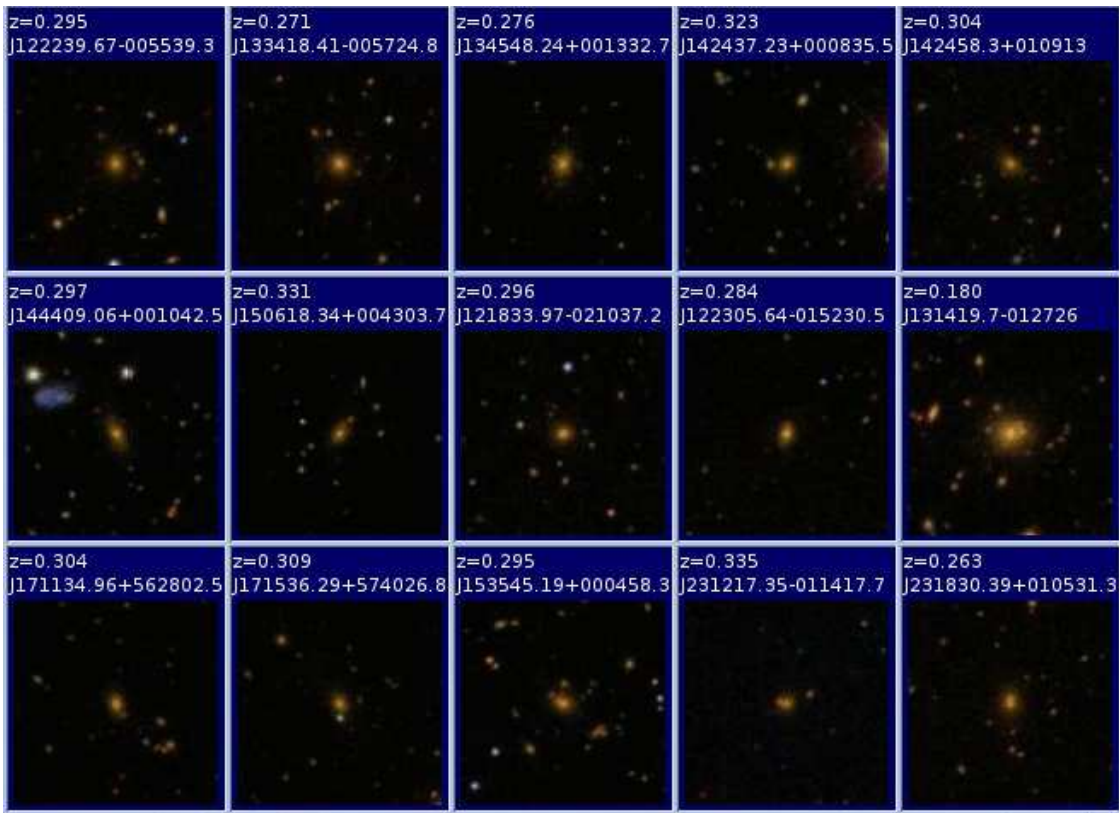


FIG. 13.— Fields centered on a random selection of objects with $M_r < -24$ in the SDSS. The fields tend to be very crowded, with many objects in the field having the same color as the central object, as expected if the central object is a BCG.

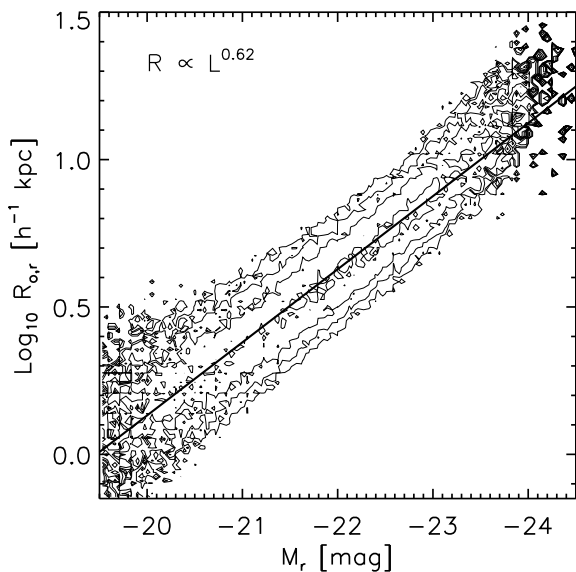


FIG. 12.— The $R_e - L$ relation defined by the bulk of the early-type galaxy population (contours). Solid line shows the power-law relation stated in the panel. At large luminosities, the true relation appears to curve upwards from this fit.

objects with $M_r < -24$ in the SDSS. The fields tend to be very crowded, with many objects in the field having the same color as the central object. This strongly suggests that the luminous central object is a BCG. Note that these are all objects at $z \sim 0.3$, so they are much more distant than the C4 BCGs we have considered so far.

6. DISCUSSION

Whether or not BCGs comprise a special population has been the subject of considerable debate for almost fifty years (Scott 1957; Sandage 1976; Schechter & Peebles 1976; Tremaine & Richstone 1977; Bhavsar & Barrow 1985; Oegerle & Hoessel 1991; Postman & Lauer 1995; Loh & Strauss 2006), with different authors coming to different conclusions. Semi-analytic galaxy formation models have long made the assumption that the central object in a halo is indeed special (Croton et al. 2005; Bower et al. 2006). And recently, halo model (see Cooray & Sheth 2002 for a review) interpretations of galaxy clustering (e.g. Zehavi et al. 2005) strongly suggest that this is indeed the case (Berlind et al. 2005; Skibba et al. 2006).

One of the reasons the subject has received so much attention (and controversy!) is that BCGs appear to be quite homogeneous—being big and bright, they may be used as standard candles out to large distances. Their attractiveness as standard candles increases if their nature is understood, since the next generation of photometric galaxy surveys will identify large numbers of clusters to redshifts of order 0.7. This means that large BCG samples

will also become available. If their nature is understood, then the BCGs themselves may provide complementary information about cosmological parameters.

BCG samples are only just becoming sufficiently large that unambiguous conclusions about their nature can be drawn. The particular question we addressed is whether or not BCG formation is dominated by dissipation or by dry mergers. The dry merger hypothesis seeks to explain why massive early-type galaxies, which are expected to have assembled their stellar mass recently, host the oldest stellar populations—even when the age estimate is luminosity-weighted. Recent observations suggest that dry mergers are a common formation mechanism for massive early-type galaxies (e.g., van Dokkum 2005). Since most BCGs are early-types, it is reasonable to ask if they show some signature of unusual formation histories.

Our analysis suggests that the answer to this question is ‘yes’. The optical surface brightness profiles of C4 BCGs appear to be of two types—one has the classical deVaucouleur profile (Figure 1), and the other shows evidence for a second, more extended, lower surface brightness component (Figure 2). The BCGs which are well-fit by classic deVaucouleur profiles have larger half-light radii than normal early-type galaxies of similar luminosities (Figure 4). The other BCGs also appear to follow a steep $R_e - L$ relation. The low surface brightness component in these objects may be due to light from the ICL. If so, then the steeper $R_e - L$ relation is also true of the BCG components of these objects, since the ICL tends to move objects along the $R_e - L$ relation, rather than change its slope (Section 4.2).

The $R_e - L$ relation of the bulk of the early-type galaxy population is steeper than the correlation between half mass radius and mass of dark matter halos. This is consistent with models in which galaxies in low mass halos have suffered more dissipation (e.g. Kormendy 1989; Dekel & Cox 2006). If massive galaxies have suffered less dissipation than less massive galaxies, then our results indicate that BCGs have suffered even less dissipation than other massive galaxies of similar luminosities.

The larger than expected sizes of BCGs suggest less dissipation, so they are consistent with the dry merger formation hypothesis. In addition, BCGs show a substantially smaller scatter around the Fundamental Plane defined by the bulk of the early-type population than does the early-type population itself (Figure 7). This might indicate that the formation histories of BCGs involve less recent star formation than occurs in early-type galaxies of similar mass; below average recent star formation rates would be consistent with dry merger formation histories.

BCGs define the same $g - r$ color-magnitude relation as the bulk of the early-type population (Figure 8). Hence, if BCGs form from dry mergers, then BCG progenitors must lie redward of this relation (else the product of the merger would lie blueward of this relation). In turn, this suggests that BCG progenitors host older stellar populations than is typical for their luminosities. This may provide an interesting constraint on dry merger models. To illustrate why, the Appendix compares our measurements with the color-magnitude relation predicted by semi-analytic galaxy formation models. The models suggest that BCGs should lie slightly blueward of the relation defined by the bulk of the

population (Figure A15)—an effect which is not seen in the data (Figure 8).

The C4 BCGs also define a tight correlation between luminosity and dynamical mass $\propto R_e \sigma^2$ (Figure 5). This, with the steeper $R_e - L$ relation, implies that they define a shallower $\sigma - L$ relation than the bulk of the population (Figure 6). Steeper $R_e - L$ and shallower $\sigma - L$ relations were also seen by Oegerle & Hoessel (1991) in their analysis of local BCG samples. However, they did not distinguish between objects which were well fit by deVaucouleurs profiles and those which were not, leaving open the possibility that the altered relations were due to inappropriate fits. This is also true of the more recent work of Lauer et al. (2006). Here we have shown that the scaling relations are altered even for objects which are well described by classical deVaucouleur profiles (Figures 4–11).

The change in slope of the $\sigma - L$ relation may be related to studies of curvature in the $M_{\text{BH}} - \sigma$ relation. This is because the most massive galaxies are expected to host the most massive black holes. This expectation is based on the strong and tight correlation between M_{BH} and the velocity dispersion σ of the spheroid/bulge which surrounds it: roughly $M_{\text{BH}} \propto \sigma^4$ (e.g. Gebhardt et al. 2000; Tremaine et al. 2002). M_{BH} also correlates with the luminosity of the bulge, although this correlation is not as tight (Magorrian et al. 1995). Recent work suggests that there is evidence for curvature in the $M_{\text{BH}} - \sigma$ relation (e.g. Wyithe 2006), in the sense that there appears to be a maximum σ beyond which M_{BH} may increase, but σ does not. This is in the same sense that we see in the $\sigma - L$ relation (Figure 6), suggesting that the masses of the most massive black holes may be better traced by bulge luminosity than velocity dispersion. This aspect of BCG properties is addressed in some detail by Lauer et al. (2006).

MB is supported by NASA grant LTSA-NNG06GC19G. We thank Tod Lauer and Mark Postman for discussions about the differences between their photometric reductions of local BCGs and those output by the SDSS pipeline, and Lucca Ciotti for discussions about dry mergers.

Funding for the SDSS and SDSS-II has been provided by the Alfred P. Sloan Foundation, the Participating Institutions, the NSF, the US DOE, NASA, the Japanese Monbukagakusho, the Max Planck Society and the Higher Education Funding Council for England. The SDSS website is <http://www.sdss.org/>.

The SDSS is managed by the Astrophysical Research Consortium (ARC) for the Participating Institutions: The American Museum of Natural History, Astrophysical Institute Postdam, the University of Basel, Cambridge University, Case Western Reserve University, the University of Chicago, Drexel University, Fermilab, the Institute for Advanced Study, the Japan Participation Group, the Johns Hopkins University, the Joint Institute for Nuclear Astrophysics, the Kavli Institute for Particle Astrophysics and Cosmology, the Korean Scientist Group, the Chinese Academy of Sciences (LAMOST), Los Alamos National Laboratory, the Max Planck Institute for Astronomy (MPI-A), the Max Planck Institute for Astrophysics (MPA), New Mexico State University, the Ohio State University, the University of Pittsburgh, the University of Portsmouth, Princeton University, the U.S. Naval Obser-

vatory, and the University of Washington.

REFERENCES

- Berlind A. et al. 2005, ApJ, 629, 625
 Bernardi M., Sheth R. K., Nichol R. C., Schneider D. P. & Brinkmann J. 2005, AJ, 129, 61
 Bhavsar S. & Barrow J., 1985, MNRAS, 213, 857
 Bower R., et al., 2006, MNRAS, in press (astro-ph/0511338)
 Boylan-Kolchin M., Ma C. & Quatert E. 2006, ApJ, submitted (astro-ph/0601400)
 Cypriano E. S., Sodr e L. Jr, Campusano L. E., Dale D. A. & Hardy E. 2006, AJ, 131, 2417
 Cooray A. & Sheth R. K. 2002, Phys. Rep., 372, 1
 Croton D., et al., 2006, MNRAS, 365, 11
 Dekel A. & Cox T. J. 2006, MNRAS, submitted (astro-ph/0603497)
 De Lucia G., et al., 2006, MNRAS, 366, 499
 Gebhardt K. et al. 2000, ApJL, 539, 16
 Gonzalez A., Zabludoff A. I. & Zaritsky, D. 2005, ApJ, 618, 195
 Hyde J., Bernardi M., et al., AJ, submitted
 Hopkins P. F., Hernquist L., Cox T. J., Di Matteo T., Robertson B., Springel V. 2006, ApJS, 163, 1
 Kodama T., Arimoto N., Barger A. J., & Aragon-Salamanca A. 1998, A&A, 334, 99
 Kormendy J. 1989, ApJL, 342, 63
 Lauer T., et al., 2006, submitted (astro-ph/0606739)
 Loh Y. S., Strauss M. A., 2006, MNRAS, 366, 373
 Magorrian J. et al. 1998, AJ, 115, 2285
 Miller C., et al., 2005, AJ, 130, 968
 Oegerle W. R. & Hoessel J. G. 1991, ApJ, 375, 15
 Postman M., Lauer T., 1995, ApJ, 440, 28
 Robinson B., Cox T. J., Hernquist L., Franx M., Hopkins P. F., Martini P. & Springel V. 2005, ApJ, 641, 21
 Sandage A., 1976, ApJ, 205, 6
 Schechter P., & Peebles P. J. E., 1976, ApJ, 209, 670
 Scott E., 1957, AJ, 62, 248
 Springel V., et al. 2005, Nature, 435, 629
 Tremaine S. D., Richstone D. O., 1977, ApJ, 212, 311
 Tremaine S. D. et al. 2002, ApJ, 574, 740
 Skibba, R., Sheth, R. K., Connolly, A. J., & Scranton, R. 2006, MNRAS, in press (astro-ph/0511773)
 van Dokkum P. G. 2005, AJ, 130, 2647
 Wyithe J. S. B. 2006, MNRAS, 365, 1082
 Zehavi, I., et al., 2005, ApJ, 630, 1
 Zibetti S., White S. S. M., Schneider D. P. & Brinkmann J. 2005, MNRAS, 358, 949

APPENDIX

COMPARISON WITH SEMI-ANALYTIC GALAXY FORMATION MODELS

The introduction states that semi-analytic galaxy formation models make strong assumptions about the formation histories of BCGs. This Appendix shows that although the models produce massive galaxies which lie on a well-defined color magnitude relation, different models disagree on the slope and zero-point of this relation (Figure A14). Nevertheless, the models do agree that the very most massive objects lie slightly blueward of the color-magnitude relation defined by the bulk of the bulge-dominated population. The SDSS early-type BCGs studied in the main text do not show such a blueward trend (Figure 8).

The ‘Munich’ and ‘Durham’ models we study here were kindly made available by Croton et al. (2005) and Bower et al. (2006) respectively. Both are based on the same underlying dark matter distribution—that of the Millennium Simulation (Springel et al. 2005). For the Durham models, we selected BCGs of halos more massive than $10^{14}h^{-1}M_{\odot}$; this resulted in about 3200 objects from a $(500h^{-1}\text{Mpc})^3$ volume. The color magnitude relation defined by these objects is shown in the left-hand panels of Figure A14.

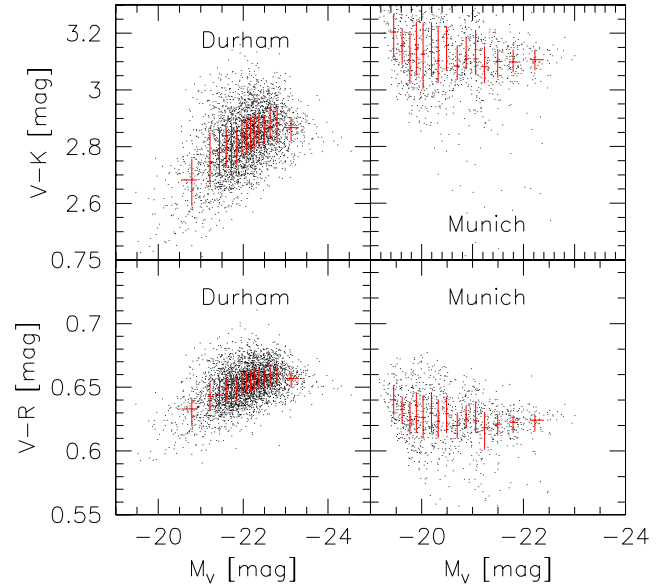


FIG. A14.— Color-magnitude relations defined by massive galaxies in the Durham and Munich semi-analytic galaxy formation models.

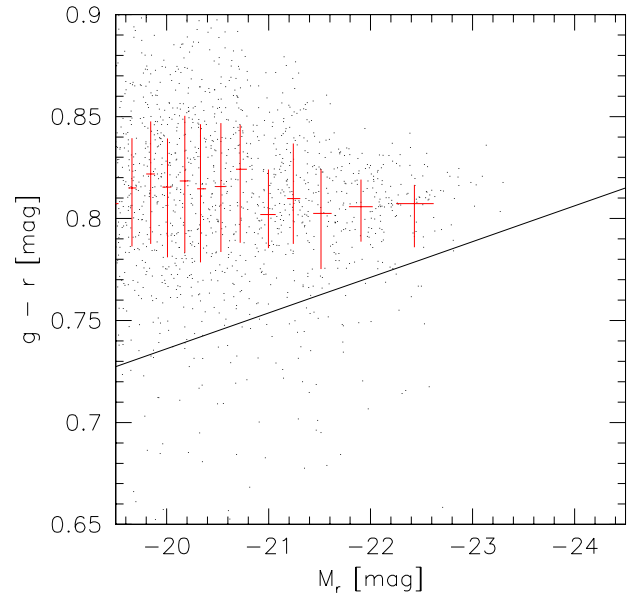


FIG. A15.— Predicted $g-r$ color-magnitude relation in the Munich model. Solid line shows the relation in the SDSS. The average color is redder than in the SDSS, and the trend for the most massive objects to be slightly bluer is not seen in the SDSS.

Selecting BCGs from the Munich models is less straightforward, because information about halo masses is not provided. However, the stellar masses of the Durham model BCGs are all greater than $1.6 \times 10^{10} h^{-1} M_{\odot}$, and so the right hand panels of Figure A14 show the color-magnitude relation of the objects which, in the Munich models, have stellar masses greater than $2 \times 10^{10} h^{-1} M_{\odot}$. The difference between the Durham and Munich models is striking, and is not particularly sensitive to this cut. This illustrates that the semi-analytic modelers have not yet converged on an unambiguous prediction for the slope and zero-point of the color-magnitude relation.

For a more direct comparison with the results presented in the main text, Figure A15 shows the predicted $g-r$ color as a function of r -band magnitude in the Munich models. Comparison with Figure 8 shows that the predicted colors are redder than in the SDSS. In addition, the trend for the most massive objects to be slightly bluer is not seen in the SDSS. If color gradients are responsible for the overall offset in color, then they must change along the color-magnitude relation to reconcile the predicted bluer colors of the most massive objects with the observations.